

## Tension Performance of Metal-Plate Connected Joints of Chinese Larch Dimension Lumber

Wei Guo,<sup>a</sup> Shasha Song,<sup>b</sup> Rongjun Zhao,<sup>a</sup> Haiqing Ren,<sup>a</sup> Zehui Jiang,<sup>b</sup> Ge Wang,<sup>b</sup> Zhengjun Sun,<sup>b</sup> Xuehua Wang,<sup>b</sup> Feng Yang,<sup>b</sup> Hong Chen,<sup>b</sup> Sheldon Q. Shi,<sup>c,\*</sup> and Benhua Fei<sup>b,\*</sup>

Tension tests of metal-plate connected (MPC) joints for Chinese larch (*Larix gmelinii* (Rupr.) Rupr.) were conducted in four orientations. Load-deflection curves were obtained for each MPC jointed specimen. Ultimate tension load, translation stiffness, stiffness at large slip, and failure modes for each specimen were obtained. A Foschi 3-parameter model was found to fit the load-deflection curves very well. Wood grain, and MPC length and loading directions had significant effects on elastic deformation and stiffness at large slip of the MPC joints. Load parallel to the grain with MPC length parallel to load (AA) represented the highest elastic deformation, while load perpendicular to the grain and MPC parallel to load (AE) showed the lowest. Load perpendicular to grain with MPC length perpendicular to load (EE) presented the highest stiffness at large slip, AA the second, load parallel to grain-MPC length perpendicular to load (EA) the third, and AE the lowest. The translation stiffness and tension load showed similar trends in terms of the effect of test orientations. The ultimate tension load was reduced by 18.9% from AA to EA, 34.2% from AA to AE, and 36.8% from AA to EE. Multiple failure modes occurred at the MPC joint, including MPC shear failure, tooth withdrawal, and wood failure.

*Keywords:* MPC joint; Translation stiffness; Ultimate tension load; Failure modes; Load-deflection curves

*Contact information:* a: Beijing Forestry Machinery Research Institute of State Forestry Administration, Beijing, 100029, China; b: International Centre for Bamboo and Rattan, No. 8 Futong Dongdajie, Wangjing, Chaoyang District, Beijing 100102, China; c: Mechanical and Energy Engineering, University of North Texas, Denton, TX 76203-1277, USA;

\* Corresponding authors: Sheldon.Shi@unt.edu, feibenhua@icbr.ac.cn

### INTRODUCTION

The metal-plate connector (MPC), invented in Florida in 1952, has been widely used in the roofing of light-frame structures. It is also referred to as a metal connector plate, truss plate, metal plate, or nail plate. The descriptive characteristics of MPC joint performance include load-deflection relation, strength, stiffness, and failure mode.

Many studies have shown that the species type significantly affects MPC performance (Quaile and Keenan 1979; Guo *et al.* 2008; Guntekin 2009). Douglas-fir, southern yellow pine (*Pinus* spp.), and SPF (spruce-pine-fir) are currently the most common species or mixtures used for MPC joints. Other species, such as spruce (mostly white spruce, *Picea glauca* (Moench) Voss) and lodgepole pine (*Pinus contorta* Dougl.), have also been reported (Lau 1987). Chinese larch (*Larix gmelinii* (Rupr.) Rupr.) is a popular species in the northeast region of China and has been used for wood frame construction because of its high strength, good decay resistance, and natural abundance.

Many tests have been conducted on the physical and mechanical properties of Chinese larch in terms of bending, compression, tension, *etc.* (Guangsheng *et al.* 2001; Wang *et al.* 2009). Guangsheng *et al.* (2001) conducted mechanical testing using small clear Chinese larch specimens with a cross section of 20 mm by 20 mm according to GB1927-1943-91 (Testing methods for physical and mechanical properties of woods) and reported that the modulus of rupture (MOR), the modulus of elasticity (MOE), and the ultimate compression strength (UCS) were 139.0 to 188.7 MPa, 4.5 to 5.0 GPa, and 42.3 to 61.1 MPa, respectively. Wang *et al.* (2009) conducted mechanical tests using full-size Chinese larch specimens with a cross section of 38 mm by 89 mm according to GB/T 50329-2002 (Standard for methods testing of timber structure) and reported MOR, MOE, 5% percentile UCS, and ultimate tension strength (UTS) values of 62.3 MPa, 13.7 GPa, 26.4 to 31.4 MPa, and 14.4 to 22.4 MPa, respectively.

Limited data have been reported on the mechanical properties of MPC joints for Chinese larch. Gupta *et al.* (1996) evaluated the strength properties of three types of mechanical connections, including MPC joint, on Russian dahurian larch (*Larix dahurica*), which comes from the same family as Chinese larch. The average ultimate 67 load for larch MPC joints was 37 kN, which was a little higher than that of southern pine 68 (28 kN) and Douglas fir (33 kN). Teeth withdrawal was found to be the only failure mode for the larch MPC joints.

Several models have been developed to describe the load-deflection behavior of an MPC joint. Foschi (1977) analyzed the MPC connections, taking into account the nonlinear characteristics of the load-deformation relationship. A nonlinear three-parameter model (see Equation 1) was developed, in which the parameters  $k$ ,  $M_0$ , and  $M_1$  were dependent on the angle between the direction of slip and the horizontal X-axis. The parameter  $k$  can be obtained from the testing of four basic plate orientations described in the Canadian standard,

$$y = (M_0 + M_1x)[1 - e^{(-kx/M_0)}] \quad (1)$$

where  $y$  is the load on the joint (kN),  $x$  is the joint displacement (mm), and  $k$ ,  $M_0$ , and  $M_1$  are parameters to be determined. In this three-parameter model,  $k$  is the initial stiffness,  $M_1$  is the stiffness at large slip, and  $M_0$  is the intercept of the asymptote with slope  $M_1$ . Gebremedhin *et al.* (1992) applied the Foschi 3-parameter model to fit the tension test data of MPC jointed specimens of southern yellow pine and showed a good fit for a single connection under an eccentric load. Amanuel *et al.* (2000) developed a two-dimensional (2D) finite-element model based on the Foschi 3-parameter model and fundamental principles of contact mechanics, only requiring basic material properties, using the commercial finite-element software ANSYS (Zhou and Guan 2008, 2011a,b). This model was able to predict the transfer of forces at the interface of a composite structure, the mechanics of tooth withdrawal, and the stiffness of tension-splice joints; the average absolute value of the error between predicted and experimental results was less than 5%. Triche and Suddarth (1988) developed a finite-element model using the frame and wood-plate elements to represent the lumber and the joint, respectively. The relative displacement between the teeth and the wood was analyzed using Foschi's equation. A good agreement between their model predictions and experimental results was reported when the displacements at selected points of the finite element model was evaluated. Gebremdhin *et al.* (1992) used a simplified two-parameter non-linear model ( $m_1 = 0$ ) to

fit the data from load-deflection characteristics of MPC joints.

The main objective of this research was to investigate the tension behavior (load-displacement curve, strength, stiffness, and failure modes) of MPC joints for Chinese larch in four orientations. Foschi's 3-parameter model was applied to fit the load-deflection curves of Chinese larch MPC joint. A comparison of MPC joint behavior was conducted between the Chinese larch and southern pine.

## EXPERIMENTAL

Chinese larch lumbers were obtained from a local wood company with a dimension of 38 mm (1.5 inches) in thickness, 89 mm (3.5 inches) in width, and 4 m (102 inches) in length. The lumbers were all IIIc grade in accordance with the Chinese standard, GB50005-2003, which is equivalent to the No. 2 grade in National Lumber Grading Authority (NLGA Standard Grading Rules for Canadian Lumber, 2003).

Gangnail GN20 metal plates with dimensions of 75 mm by 100 mm (3 × 4 inch) and 75 mm by 125 mm (3 × 5 inch) were obtained from a local manufacturer. One piece of 600-mm-long lumber was cut in half, and the two halves were jointed with MPCs on both sides with a hydraulic machine to fabricate a MPC joint specimen. All the MPC jointed specimens were placed in laboratory conditions for 1 week before testing in accordance with the procedure described in ANSI/TPI1-2002, CAS-S347-99.

Specimens with four joint orientations were prepared for testing: load parallel to grain, MPC length parallel to load (AA orientation); load parallel to grain, MPC length perpendicular to load (EA orientation); load perpendicular to grain, MPC parallel to load (AE orientation); and load perpendicular to grain, MPC length perpendicular to load (EE orientation) (ANSI/TPI1-2002, CAS-S347-99). MPCs 75 mm (3 inches) wide and with a length of 100 mm (4 inches) for the EE orientation and 125 mm (5 inches) for the AA, EA, and AE orientations were used to prepare the MPC jointed specimens.



**Fig. 1.** MPC joint test setup

Tension tests were conducted using a universal test machine with a capacity of 50 kN. The cross head movement was about 1 mm/min, so that the specimens failed in 5 min. The relative axial displacement of each specimen was recorded by a pair of linear variable differential transformers (LVDTs) placed on two sides of the MPC joint. The load and displacement data were collected by a data acquisition system until failure. Two 20-mm-diameter holes were predrilled along the specimen width at both ends of the MPC jointed specimen at a location 100 mm away from the end. Two steel bars were inserted into the holes, through which the tensile load was applied to the MPC joint specimen in a universal testing machine. The detailed testing set-up is shown in Fig. 1.

The stiffness of the MPC joint specimens was determined in two ways. One was to calculate stiffness from the slope of the load-deflection curve at the allowable design load, which was defined as the ultimate load divided by 3 (a factor considering load duration and safety). The other calculated the stiffness by dividing the load at the critical slip (= 0.38 mm) by 0.38 mm (TPI 1985).

Moisture content (MC), air-dry density, bending strength, and modulus of elasticity (MOE) of the larch dimension lumber were obtained in accordance with the procedures described in Chinese Standards GB/T1931-1991, GB/T1933-1991, and GB50329-2002. Dynamic MOE was also calculated based on the frequency data obtained from the longitudinal vibration at a base frequency using an AD3542 FFT Analyzer.

## RESULTS AND DISCUSSION

### Material Properties

The physical and mechanical properties of Chinese larch are shown in Table 1 in a comparison with southern pine. As shown in Table 1, the average density of Chinese larch dimension lumbars was measured as 0.65 g/cm<sup>3</sup>, which is higher than that of southern pine. The moisture content (MC) of the lumber was 12%. The average modulus of elasticity (MOE) of dahurian larch was reported as 12.1 GPa by Gupta and Vatovec (1996), which was slightly lower than that for the Chinese larch used in this research (13.8 GPa).

Both the dynamic and static MOEs of Chinese larch were all slightly higher than that of southern pine, while the bending strength was lower (Table 1). Usually, materials with a high stiffness also present a high strength (Bodig and Jayne 1993). The abnormally high stiffness with low strength phenomenon for the Chinese larch could be due to small knots and potential splits.

### Analysis of the Load-Deflection Curves

Figure 2 shows the load-deflection curves of the MPC jointed specimens at four different orientations. The tensile load-deflection curves of Chinese larch MPC jointed specimens exhibited a nonlinear relationship. The Foschi nonlinear three-parameter model (Equation 1) was applied to fit to all the load-deflection data of the MPC specimens at the same time. Each experimental data set was fitted with this non-linear curve by Origin Pro 7.5 software (Fig. 2).

**Table 1.** Property Comparison between Chinese Larch and Southern Pine

Physical and mechanical index\tree species	Chinese larch #	Southern pine
MC*	12%	10%(COV=3.5) (Gupta <i>et al.</i> 1992, Gupta and Gebremedhin 1989, McLain <i>et al.</i> 1984) 12% (McCarthy and Wolfe 1987)
Air-dry density	0.65g/cm <sup>3</sup> (0.5-0.88)	SG=0.48 (COV=14.6%) (Gupta and Gebremedhin 1989) SG=0.52 (0.37-0.70) (McCarthy and Wolfe 1987) SG=0.55-0.57 (Via <i>et al.</i> 1999) SG=0.49 (Groom 1994)
Dynamic MOE	15.1 GPa (COV=17.35%, n=160)	MOE <sub>(CLT)</sub> =11.7GPa(6.9-17.2) ( McCarthy and Wolfe 1987) MOE <sub>(MSR)</sub> =12.4-13.1GPa (Via <i>et al.</i> 1999)
Static MOE	13.8 GPa (COV=18.39%, n=160)	9.7GPa (COV=25%,n=250) (Gupta 1992) 11.2GPa (COV=27.7%,n=99) (McLain 1984) 12.1GPa (Groom 1994)
Bending strength	62.3 MPa (COV=34.05%, n=160)	59.6MPa (COV=43.6%,n=99) (McLain 1984)
Tension strength	--	33MPa (COV=46.8%,n=98) (Showalter <i>et al.</i> 1987)

\*Moisture content measured from a 38 mm by 89 mm wood block from the MPC-jointed specimen immediately after testing; # tested in the present study

The following equations were obtained for each orientation.

$$\text{AA orientation: } y = (26.73+6.11x) [1-e^{(-149.86x/26.73)}] \quad (2)$$

$$\text{EA orientation: } y = (23.78+2.27x) [1-e^{(-142.38x/23.78)}] \quad (3)$$

$$\text{AE orientation: } y = (22.30+0x) [1-e^{(-81.20x/22.30)}] \quad (4)$$

$$\text{EE orientation: } y = (15.24+8.50x) [1-e^{(-104.08x/15.24)}] \quad (5)$$

According to the load-deflection curve fitting, the  $R^2$  values for the Foschi model fit of the experimental data in four orientations were obtained as 0.98 for AA, 0.99 for EA, 0.91 for AE, and 0.85 for EE, indicating that the Foschi model is a good predictor of the load-deflection curve of MPC jointed Chinese larch specimens for AA, EA, AE three orientation.

As shown in Fig. 2, the initial stage of the load-deflection curve that was not more than 10 KN was nearly linear, which reflected the property of the initial stiffness,  $K$  (KN/mm). The steeper the slope for the linear section, the higher the  $K$  and the stronger the resistance to elastic deformation. In the testing of MPC jointed Chinese larch, the parameter  $K$  was measured as 149.9 for AA, 142.4 for EA, 104.1 for EE, and 81.2 for AE. The slope of the load-deformation curve at the later stage,  $M_1$ , represented the

stiffness property at a higher deflection, and the values of  $M_1$  were obtained as 8.5 for EE, 6.1 for AA, 2.3 for EA, and 0.0 for AE (Fig. 2). From the Foschi model fit, the highest slope of the curve at the later stage was obtained for the EE orientation (highest resistance to deformation), indicating that the EE orientation provided the highest resistance to the deformation among the four orientations tested. When this slope is close to zero (see AE orientation), a simplified 2-parameter equation can be used to fit the load-deflection curve.

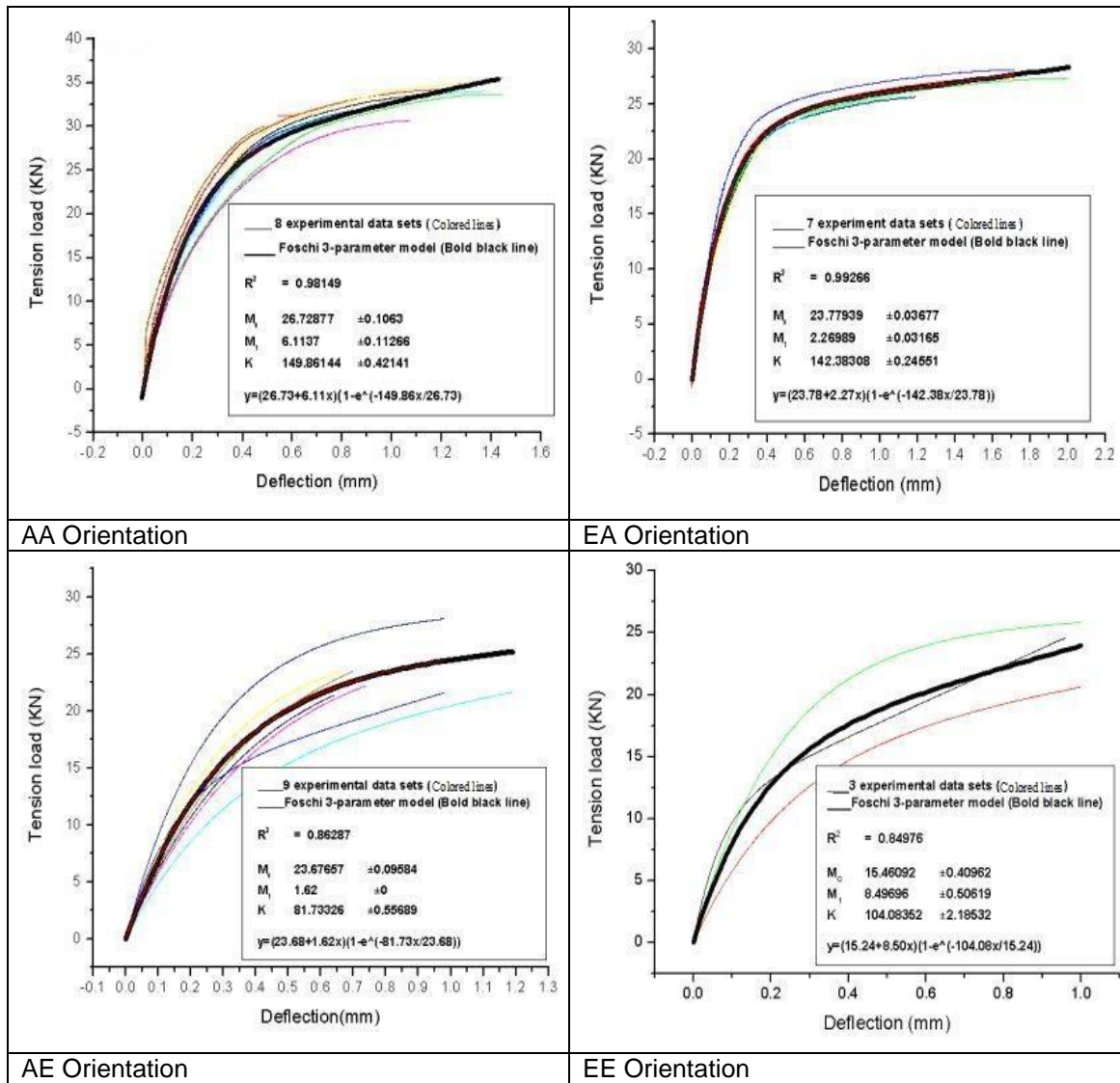


**Fig. 2.** Load-deflection curves and the Foschi model fit for MPC jointed Chinese larch in four orientations

Figure 2 also demonstrates that the variation among the replications for the load-deflection curves for the AA orientation was the smallest, while that for the EE orientation was the largest. This phenomenon could be attributed to the different wood grain arrangements in the two halves of the joint. For AA and EA orientations, the wood

grains are parallel to each other. For AE and EE orientations, the wood grains are perpendicular to one another.

### Tensile Properties

The average ultimate tensile loads were measured as 32.7 kN for AA, 26.6 kN for EA, 21.5 kN for AE, and 20.7 kN for EE. The ultimate tensile load decreased by 18.9% from AA to EA, by 34.2% from AA to AE, and by 36.8% from AA to EE. These decreases may be due to the different interaction forces between the teeth and the wood. When the MPC joint was in the AA orientation, wood fibers were cut by teeth and the compression load was the dominant interaction between the wood and the teeth. In the EA orientation, wood fibers were torn by the teeth during the loading. However, no weak point was present for the whole sample with the wood grains in one direction. In the AE orientation, the wood fibers of one half were in compression, while the other half were in both compression and tearing. The half with the tearing was weaker, which would cause the failure. In the EE orientation, wood fibers of both halves were in shear. The half of the wood grain that was perpendicular to the tensile load was weaker. From the above analysis, it is concluded that the MPC joint represents a high ultimate tensile load when compression dominates between teeth and wood fibers and a low tensile load when tear or shear force dominates. The half of the specimen with weaker load bearing will accelerate the process of failure. For the AA orientation, the ultimate tensile load of Chinese larch was lower than that of dahurian larch, which is 37 kN (8,190 pounds) (Gupta and Vatovec 1996), but a little higher than that of southern pine (Gupta *et al.* 1992, Gupta and Gebremedhin 1989, Groom 1994). This comparison of ultimate tensile load on MPC joints is similar to that of the strength of Chinese larch, which was higher than that of southern pine. The maximum deflection at the failure was measured as 0.69 to 2.04 mm.

The translational stiffness reflects the ability of the MPC joint to resist axial deformation. The translational stiffness is usually obtained from the load at the critical slip of 0.38 mm divided by 0.38 mm from the tensile load-deflection curves (TPI 1985, Gebremedhin *et al.* 1992). In the present tests, the translation stiffness was 27.6 kN/mm for AA, 22.8 kN/mm for EA, 16.0 kN/mm for AE, and 15.9 kN/mm for EE. As shown in Table 2, except for the AE orientation, the translational stiffness for the other three orientations were lower than that of southern pine (39.9 kN/mm for AA, 20.5 kN/mm for EA, and 23.0 kN /mm for EE). The load at the critical slip of 0.38 mm for the southern pine load-deflection curve was generally higher than that of Chinese larch, according to the definition of translation stiffness. Thus, it can be deduced that Chinese larch has a higher stiffness than southern pine, considering the lower translation stiffness with the higher ultimate tensile load.

The initial stiffness ( $K$ ) obtained for the Chinese larch were much higher than those measured by McCarthy and Wolf (1987) for southern pine (Table 2). As shown in Table 2, both translational stiffness and initial stiffness for the MPC jointed Chinese larch show a decreasing trend from AA, EA, AE, to EE. It can also be seen that Chinese larch presents a higher tensile strength and initial stiffness, but a lower stiffness at critical slip, compared with southern pine.

### Failure Modes of MPC Joint Tested in Tension

Figure 3 shows that four primary failure modes were observed in the tension test for the MPC jointed Chinese larch specimens: (1) MPC shear failure, (2) tooth withdrawal, (3) wood failure, and (4) combination of the three. Tooth withdrawal and MPC failure were most prevalent.

**Table 2.** A Comparison of Tension Properties of MPC Joint between Chinese Larch and Southern Pine

Tree Species	Property Index	Values of Four Joint Orientation			
		AA	EA	AE	EE
Chinese larch	Plate size (mm)	75×125	75×125	75×125	75×100
	Ultimate tensile load (KN)	32.73	26.55	21.52	20.68
	Initial stiffness (KN/mm)	149.86	142.38	81.20	104.08
	Stiffness at critical slip (KN/mm) #	27.61	22.79	16.01	15.90
	Failure mode	MPC failure wood failure	MPC failure	Tooth withdr. wood failure	MPC failure, wood failure
Southern pine (Gebremedhin 1992)	Plate size (mm)	75×125	75×125	75×125	75×125
	Ultimate tensile load (KN) *	26.03	12.43	19.05	14.08
	Displacement at failure (mm) *	1.62	1.71	1.24	1.50
	Stiffness at critical slip (KN/mm)	39.88	20.48	26.79	22.98
	Failure model	MPC shear wood failure	Tooth withdraw	Wood failure, tooth withdr.	Tooth withdrawal
Southern pine (McCarthy 1987)	Plate size (mm)	75×125	75×125	75×125	75×125
	Ultimate tensile load (KN)*	14.47	15.47	7.89	13.70
	Init. stiff. (KN/mm)	114.29	117.86	37.86	48.40
	Failure model	Over 90% tooth withdrawal, the rest wood failure or a combination of tooth withdrawal and wood failure.			

\*average value; # critical slip is stated to 0.015 inch



Tooth withdrawal

MPC failure

Wood failure A





Wood failure B

Wood failure with tooth withdrawal

Tooth withdrawal with wood failure

**Fig. 3.** Failure modes of Chinese larch MPC joints in tension tests

Tooth withdrawal was evident mainly for the joints in AA and EA orientations. For the joints in AE and EE orientations, failure usually occurred in the wood member in the horizontal grain direction. These members were subjected to a force perpendicular to the grain. Most of the joints in AA and EA orientations failed due to the plate shear. Tension parallel to the grain was greater than the shear of the MPC at the critical section. The MPC was sheared in half at the joint interface where the teeth were punched.

For the AA orientation, two types of failure modes, plate failure and wood failure, were presented in Chinese larch. The same failure modes were also observed for southern pine (Gebremedhin *et al.* 1992). For the EA orientation, the failure modes among the MPC joints were similar to each other, while the failure modes of the other three orientations were complicated (Table 2).

Tooth withdrawal failure was prevalent in this research. The failure appeared at the weakest point in the middle of the MPC, the slot, when the MPC length was 100 mm. The failure mode was more complex when there was no slot in the middle of the MPC. Therefore, the ultimate tensile load of joints with 75 by 100 MPC might not necessarily be less than that with 75 by 125 MPC. As can be seen in Table 2, the ultimate tensile load of MPC jointed Chinese larch specimens in the EE orientation was 20.7 kN, which was higher than that of southern pine using 75 by 125 MPC. The EE orientation showed a similar result to that in the AE orientation for the Chinese larch specimens. Figure 3 shows some of the failures for the MPC jointed Chinese larch specimens. For Chinese fir, more brittle failure was observed with such wood failure modes.

## CONCLUSIONS

1. The Foschi 3-parameter model was successfully applied to the load-deflection curves of MPC joints for Chinese larch with  $R^2$  values of 0.85 to 0.98 for four orientations. The initial stiffness and the stiffness at large slip were obtained from the fitting curves.
2. The initial stiffness showed a decreasing trend from the orientation AA, to EA, to EE, and to AE. The stiffness at large slip reduced from the orientation EE to AA to EA and to AE.

3. The average ultimate tensile loads were decreased by 18.9% from AA to EA, by 34.2% from AA to AE, and by 36.8% from AA to EE. The MPC joint possessed a high tensile load when compression dominated the interaction force between the tooth and wood fibers and a low tensile load when tear or shear force dominated.
4. For the translation stiffness and the ultimate tensile load of the MPC jointed Chinese larch, the AA orientation presented the highest value among the four orientation joints. Chinese larch presented a higher tensile strength and initial stiffness of the MPC joints compared with those of southern pine.
5. Complicated failure modes occurred for the MPC joint of Chinese larch in tension tests, including (1) MPC shear failure, (2) tooth withdrawal, (3) wood failure, and (4) a combination of (1)-(3). Tooth withdrawal and MPC failure were predominant. From the failure modes, the Chinese larch was well suited to sustain tension, and should not be evaluated as a T-test specimen. Chinese larch as a plantation forest can partly replace natural forest in light wood frame or imported materials.

## ACKNOWLEDGMENTS

This study was funded by the National forestry public welfare industry specific research project “Research and demonstration of manufacture key techniques for larger span bamboo engineering components” (201204701) and the state “The Twelfth Five-Year” science and technology support projects “Research and demonstration of manufacture techniques for green bamboo rattan building materials” (2012BAD23B01).

## REFERENCES CITED

- Amanuel, S., Gebremedhin, K. G., Boedo, S., and Abel, J. F. (2000). “Modeling the interface of metal-plate-connected tension-splice joint by finite element method,” *Transactions of the ASAE* 43(5), 1269-1277.
- Bodig, J., and Jayne, B. A. (1993). *Mechanics of Wood and Wood Composites*, Reprinted edition, Krieger Publishing Company, Malabar, Florida.
- Canadian Standards Association. (2004). “Method of test for evaluation of truss plates used in lumber joints,” CSA Standard S347-99.
- Foschi, R. O. (1977) “Analysis of wood diaphragms and trusses Part II: Truss-plate connections,” *Canadian J. Civil Eng.* 4(3), 353-362.
- Gebremedhin, K. G., Jorgensen, M. C., and Woelfel, C. B. (1992). “Load-slip characteristics of metal plate connected wood joints tested in tension and shear,” *Wood and Fiber Science* 24(2), 118-132.
- Groom, L. H. (1994). “Effect of moisture cycling on truss-plate joint behavior,” *Forest Products Journal*, 44(1), 21-29.
- Guangsheng, C., Hongqing, Y., and Shufen, Z. (2001). “Comparison on physical mechanics property of larch wood in different planting density,” *Journal of Northeast Forestry University* 29(3), 7-12.
- Guntekin, E. (2009). “Performance of Turkish Calabrian pine timber joints constructed with metal plate connectors ,” *Wood Research* 54(3), 99-108.

- Guo, W., Fei, B., Zhao, R., and Zhou, H. (2008). "Review of tests and impact factors of metal-plate connection," *China Wood Industry* 22(6), 24-27.
- Gupta, R., and Vatovec, M. (1996). "Evaluation of dahurian larch in mechanical connections," *Forest Products Journal* 46(9), 89-93.
- Gupta, R., Gebremedhin, K. G., and Grigoriu, M. D. (1992). "Characterizing the strength of wood truss joints," *Transactions of ASAE* 35(4), 1284-1290.
- Gupta, R., and Gebremedhin, K. G. (1989). "Destructive testing of metal-plate-connected wood truss joints," *Journal of Structural Engineering* 116(7), 1971-1982.
- Gupta, R., Ethington, R. L., and Green, D. W. (1996). "Mechanical stress grading of dahurian larch structural lumber," *Forest Products Journal* 46 (7/8), 79-86.
- Lau, P. W. C. (1987). "Factors affecting the behaviour and modelling of toothed metal-plate joints," *Canadian Journal of Civil Engineering* 14(2), 183-195.
- McCarthy, M., and Wolfe, R. W. (1987). *Assessment of truss plate performance model applied to southern pine truss joints*, Research Paper FPL-RP-483, USDA, Forest Products Laboratory, Madison, WI.
- McLain, T. E., DeBonis, A. L., Green, D. W., Wilson, F. J., and Link, C. L. (1984). "The influence of moisture content on the flexural properties of southern pine dimension lumber," No. FSRP-FPL-447. Forest Products Laboratory, Madison, WI.
- Quaile, A. T., and Keenan, F. J. (1979). "Truss plate testing in Canada: Test procedures and factors affecting strength properties," *Proceedings of Metal Plate Wood Truss Conference*, Forest Products Society, Madison, WI, 105-112.
- Showalter, K.L., Woeste, F.E., and Bendtsen, B.A. (1987). *Effect of length on tensile strength in structural lumber*, Research Paper FPL-RP-482, USDA, Forest Service, Forest products Laboratory, Madison, WI.
- Triche, M. H., and Suddarth, S. K. (1988). "Advanced design of metal plate connector joints," *Forest Products Journal* 38(9), 7-12.
- Truss Plate Institute (1985). *Design specifications for metal-plate connected wood trusses*, Truss Plate Institute, Inc., Madison, WI.
- Truss Plate Institute (2002). "Performance evaluation of metal connector plated connections," *ANSI/TPI 1-2002*, 22-38.
- Via, B. K., Zink-Sharp, A., Woeste, F. E., and Dolan, J. D. (1999). "Relationship between tooth withdrawal strength and specific gravity for metal plate truss connections," *Forest Products Journal* 49(7/8), 56-63.
- Wang, Z., Ren, H., Luo, X., and Zhou, H. (2009). "Mechanical stress of larch dimension lumber from Northeastern China," *China Wood Industry*, 23(3), 1-4.
- Zhou, T. and Guan, Z. W. (2008). "Rational designing of double-sided nail plate joints using finite element method," *International Journal of Structural Engineering and Mechanics* 28(2), 239-257.
- Zhou T., and Guan, Z. W. (2011a). "A new approach to obtain flat nail embedding strength of double-sided nail plate joints," *Construction and Building Materials* 25(2), 596-607.

Zhou, T., and Guan, Z. W. (2011b). “Numerical modeling for sensitivity analysis of wood joints made with double-sided punched metal plate fasteners,” *Advances in Structural Engineering* 14(2), 163-178.

Article submitted: April 25, 2013; Peer review completed: June 16, 2013; Revised version received: September 15, 2013; Accepted: September 16, 2013; Published: September 23, 2013.